Modular Ligation of Thioamide Functional Peptides onto Solid Cellulose Substrates

Thomas Tischer, Anja S. Goldmann, Katharina Linkert, Vanessa Trouillet, Hans G. Börner, and Christopher Barner-Kowollik**

Hetero Diels-Alder (HDA) cycloaddition – as an effective modular conjugation approach – is employed to graft thioamide endfunctional oligopeptides onto solid cyclopentadienyl (Cp) functional cellulose substrates generating cellulose-peptide hybrid materials. The highly reactive Cp moieties serve as diene functionality in the consecutive HDA reaction on the biosubstrate surface. Oligopeptides (i.e., the model peptide Gly-Gly-Arg-Phe-Pro-Trp-Trp-Gly and the antimicrobial peptide tritrpticin) are functionalized at their N-termini employing strongly electron deficient thiocarbonyl thio compounds resulting in biomacromolecules bearing a thioamide endgroup. The dienophile-functional peptides readily undergo HDA reactions at ambient temperature and under mild conditions in solution with synthetic polymers as well as on solid (bio)substrates. An in-depth investigation is provided of the influence of the temperature, the Lewis acid catalysis and the side group exchange of thioamide functional oligopeptides reacting with Cp terminated poly(methyl methacrylate) (M_n = 2100 g·mol^{-1}, *PDI* = 1.1) in homogenous solution as well as Cp functionalized cellulose in a heterogeneous system. To assess the success of the grafting reaction, the soluble samples were subjected to characterization methods such as size exclusion chromatography (SEC) and SEC-electrospray ionization mass spectrometry (SEC-ESI-MS). The heterogeneous "grafting-to" reactions were monitored using high resolution attenuated total reflection (ATR) Fourier transform infrared microscopy (HR-FTIRM) imaging, X-ray photoelectron spectroscopy (XPS) and elemental analysis. Evaluation via elemental analysis leads to quantitative peptide cellulose surface loading capacities.

1. Introduction

Altering the properties of materials originating from natural resources is one of the most challenging tasks undertaken by material scientists. The role of biopolymers in current polymer research is steadily increasing. Cellulose – as one of the most abundant renewable biosubstrates, with an annual natural production close to 10^{12} t – with its available functional groups for subsequent modifications is thus a versatile template in biocompatible material science.[1] Modification of cellulose can be achieved using homogeneous[2] or heterogeneous[3] approaches. In the present study, the heterogeneous route was chosen since it allows for easy processing (i.e. no precipitation) of the sample.

Grafting approaches are one of the most common methods to tailor material properties.[4] The "grafting-to" approach utilizes pre-made polymer or peptide strands to graft them onto a (functional) surface.[5] If entities are grown directly from the surface one refers to a "grafting-from" approach. The latter is the more common since it can lead to high grafting densities.[1c,6] Nevertheless, there are specific advantages of the grafting-to approach which play a pivotal role in the current study. Especially when employing a highly effective grafting method, grafting densities comparable to those obtained in 'grafting-from' approaches are achieved.[7] The synthesis of tailored polymer strands for tethering them onto the surfaces allows for an intensive characterization prior to attachment, for example via size exclusion chromatography (SEC), nuclear magnetic resonance spectroscopy (NMR) or electron spray ionization mass spectrometry (ESI-MS) resulting in a clear image of the species that are to be grafted onto the surface. In a previous publication the successful 'grafting-to' approach of poly(iso bornylacrylate) on Cp functionalized cellulose surfaces utilizing reversible-addition fragmentation chain transfer-hetero Diels-Alder (RAFT-HDA) chemistry was reported.[8]

Our current efforts are directed at not only showing the in-principle feasibility of attaching synthetic polymer chains to solid cellulose substrates, but rather aim at providing a practical

T. Tischer, Dr. A. S. Goldmann, Prof. C. Barner-Kowollik
Preparative Macromolecular Chemistry
Institut für Technische Chemie und Polymerchemie
Karlsruhe Institute of Technology (KIT)
Engesserstr. 18, 76128 Karlsruhe, Germany
E-mail: christopher.barner-kowollik@kit.edu
K. Linkert, Prof. H. G. Börner
Laboratory for Organic Synthesis of Functional Systems
Department of Chemistry
Humboldt-Universität zu Berlin
Brook-Taylor-Str. 2, 12489 Berlin, Germany
E-mail: h.boerner@hu-berlin.de
V. Trouillet
Institute for Applied Materials (IAM-WPT)
Karlsruhe Institute of Technology (KIT)
Hermann-von-Helmholtz-Platz 1,
76344 Eggenstein-Leopoldshafen, Germany

DOI: 10.1002/adfm.201200266

and robust 'grafting-to' pathway for the attachment of model and functional peptide sequences to cellulose.

However, RAFT agents are frequently prone to reactions with nucleophiles e. g. amines,[9] which limits the possibility to ligate peptides. To ensure the robustness and bioorthogonality of our novel approach, we purposefully equip peptide strands with HDA capable thioamides instead of dithioester entities to reduce any occurrence of hydrolysis and to prevent side reactions. Thus, variable peptide sequences were functionalized with electron deficient thioamide entities which can undergo HDA reactions under mild conditions with suitable dienes. The thioamide functional peptides were subsequently utilized in conjugation reactions with Cp terminated polymers as model systems as well as Cp functionalized cellulose surfaces. Specifically tritrpticin was successfully grafted onto cellulose, a peptide which is known to show antimicrobial activity also in its surface bound state.[10] The overall peptide cellulose design strategy followed in the present study is depicted in **Scheme 1**.

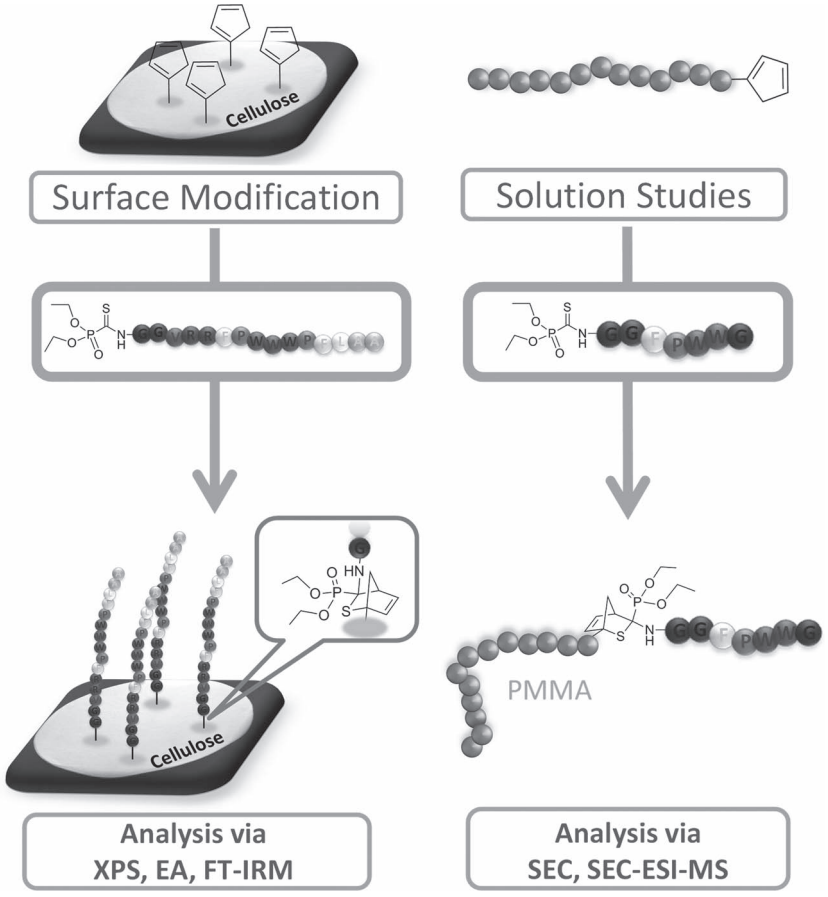

Scheme 1. Schematic representation of the two-pronged research strategy employed in the current study: Ligation assessment via thioamide functional peptides in solution and functional peptide (tritrpticin) grafting onto solid cellulose substrates via mild hetero Diels-Alder (HDA) chemistry. The ligation success is evaluated by a range of analytical techniques, including high resolution IR imaging.

2. Results and Discussion

The biopolymer cellulose is built of D-glucose units which are connected by β-1,4-glycosidic linkages.[4] The monomer unit contains one primary and two secondary hydroxyl groups. The presence of the hydroxyl group leads to strong inter- and intramolecular hydrogen bonds, resulting in a semicrystalline structure.[11] Three main sources for cellulose are available, i.e. wood, cotton and bacteria.[4] Current cellulose research is focused on different morphologies, for example microfibrillated[12] or nanocrystalline[13] cellulose. In the present study filter paper manufactured from cotton (Whatman No.5) was employed because of its facile accessibility. As grafting method the highly effective HDA cycloaddition was selected thus following a grafting-to approach. As noted in the introduction, 'grafting-to' approaches have been reported as sometimes yielding lower grafting densities compared to grafting-from approaches,[14] although recently 'grafting-to' systems have also been reported that lead to high substrate loading capacities.[7] Tailor-made peptides with the ability to undergo HDA reactions were obtained by functionalization of the peptide termini with HDA-capable electron deficient thiocarbonyl thio compounds.

The synthesis of two peptide sequences was performed in a fully automated manner applying solid-phase supported peptide synthesis (SPPS) procedures with the Fmoc/*t*Bu strategy. Both the model sequence Gly-Gly-Arg-Phe-Pro-Trp-Trp-Gly (GGF-PWWG), which constitutes a section of the antimicrobial peptide tritrpticin and the full tritrpticin sequence GGVRRFPWW-WPFLAA (please refer to Figure S8 for the chemical structure of tritrpticin) were elongated with a N-terminal GG insert. At supported peptides the introduction of the HDA-active moiety could be performed, preserving the ease of purification of the solid-phase supported synthesis procedure. The N-terminal amino group reacts under slightly basic condition cleanly with the benzyl(diethoxyphosphoryl)dithioformiate (BDPDF). The aminolysis of BDPDF leads to the quantitative formation of a N-terminal thioamide end-functionality of the peptides. The thioamide endgroup is stable under harsh acidic conditions (e.g. TFA 90%, 1 h) and thus survived the cleavage conditions allowing to isolate the fully deprotected peptides. ESI-MS experiments proved the chemical nature of the compounds and evidenced a clean synthesis of the desired thioamide-functional peptides via the absence of side products.

To the best of our knowledge there are three species of thiocarbonyl thio compounds available – which can also act as RAFT agents – known to undergo [4 + 2] cycloaddition reactions under mild reaction conditions due to their electron-withdrawing Z-group.[7a,15] For example benzyl pyridine-2-yldithioformiate (BPDF) reacts with reactive dienes after activation with trifluoroacetic acid. It could be shown that BPDF allows conjugation of

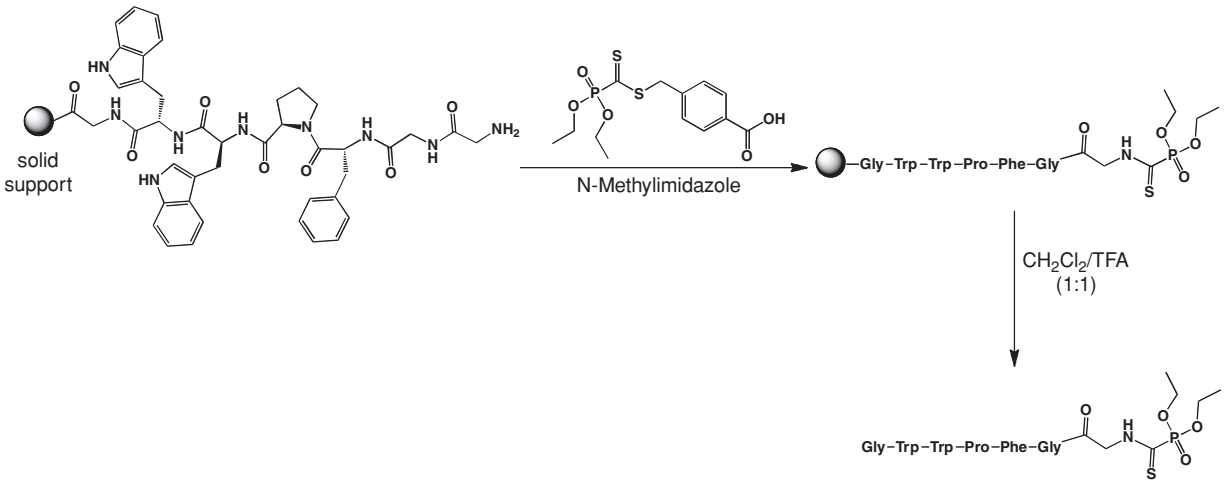

Scheme 2. Solid supported synthesis of a thioamide functionalized oligopeptide (Phos-GGFPWWG) via aminolysis of BDPDF derivative and subsequent cleavage from the solid support.

polymers onto biosubstrates,[8] the formation of block copolymers[15] as well as the construction of star polymers[16] as long as a reactive diene is present. Equipped with a sulfonyl moiety as Z-group, thiocarbonyl thio entities are known to be very reactive[17] even towards monomer species such as methyl methacrylate and styrene. Their very high reactivity makes them difficult to handle and thus to obtain a compromise between reactivity and usability the third dienophilic species was chosen: Benzyl(diethoxyphosphoryl)dithioformiate (BDPDF), whose derivatives are known to undergo HDA reactions without the need for a catalyst. Synthetic (glyco)polymers prepared on the basis of B(D)PDF were already successfully grafted onto microspheres.[7b,18] Peptides N-terminally functionalized with electronrich C=S double bond thiocarbonyl thio termini – not thioamide chain ends – have been reported. They were synthesized via amide formation between a terminal amine moiety of the peptide and a carboxy moiety of a RAFT agent. The resulting 'macro-chain transfer agents' (macro-CTAs) are known to be effective to mediate the RAFT polymerization yielding biohybrid polymers (bioconjugates).[9] The present study follows a related approach starting from a dithioester yet resulting in a more robust (see above) thioamide functional oligopeptide rather than a 'macro-CTA'. The thioamide functionalized peptide cannot be used – in contrast to the above mentioned peptide-RAFT agents – to control a radical polymerization process but instead functions as a HDA active linker in the subsequent conjugation reaction. **Scheme 2** depicts the functionalization procedure of the model oligopeptide Gly-Gly-Arg-Phe-Pro-Trp-Trp-Gly with a BDPDF derivative. Although the initial thiocarbonyl thio species bears a carboxy functionality, the reaction pathway of aminolysis is favoured because the electron withdrawing Z-group is leaving the dithioester moiety more assailable to nucleophilic attack. The thioamide functional oligopeptide (**2**) was subsequently investigated with respect to its ability to undergo [4 + 2] cycloadditions. To evaluate the reaction conditions under which the best conversion can be observed, a model study with Cp terminated poly(methyl methacrylate) (PMMA-Cp, **1**) was carried out in solution and characterized by SEC and SEC-ESI-MS (**Scheme 3**). Investigations were carried out concerning the HDA reactivity of a thioamide functional oligopeptide similar to those species resulting from a RAFT-HDA process, although the R-group and the adjacent sulfur were substituted (see Scheme 2). To demonstrate that the HDA reaction is connecting the peptide to the diene, similar reaction conditions were chosen – in particular ambient temperature and mild reaction conditions – to allow comparability to the classical RAFT-HDA process.[8,18,19] Since the RAFT-HDA reaction showed excellent conversion in chlorinated solvents, the current reactions were also carried out in $CHCl_3$.[20] It is known that trifluoroacetic acid (TFA) is accelerating the reaction if the RAFT-group is bearing a pyridinyl moiety. In the present study, TFA is added merely to improve the solubility of the thioamide functionalized peptide.

The influence of the TFA concentration on the conversion can be clearly visualized when inspecting the integration ratio obtained from SEC-ESI-MS experiments of product and reactant signal (refer to **Figure 1**). Information on how mass spectrometry on the forming oligopeptide synthetic hybrid polymer material can lead to quantitative reaction rate data is provided in the experimental section. It is evident that a sufficient

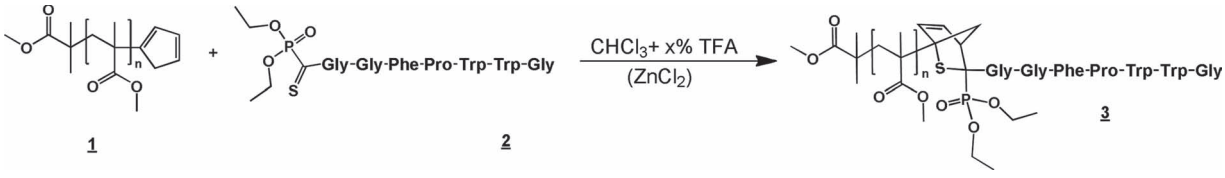

Scheme 3. General strategy for the coupling of the thioamide functional peptide (Phos-GGFPWWG) and cyclopentadienyl terminated polymer in homogenous solution: PMMA-*b*-GGFPWWG as a model system.

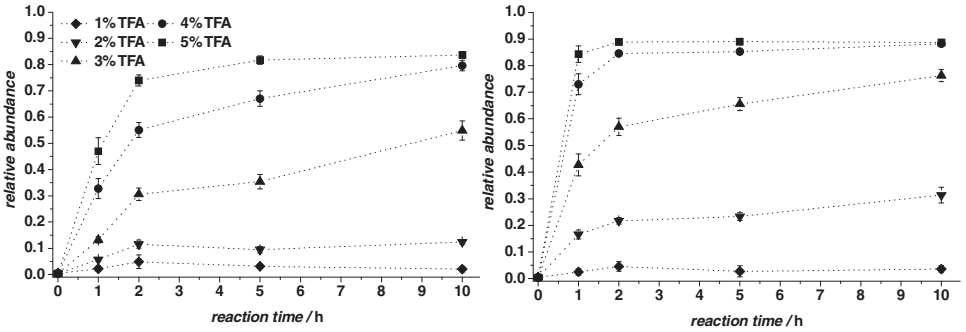

Figure 1. Variation of the TFA concentration and the influence of Lewis acid catalysis ($ZnCl_2$) on the conversion in model peptide-synthetic polymer solution ligation experiments visualized via the integration ratio of the product (**3**)/reactant (**1**) signal resulting from a SEC-ESI-MS experiment for the elution time segment between 15.2–16.6 min of three repeating units as a function of the reaction time. Typical primary SEC-ESI-MS data can be viewed in Figure S5. The variation of the TFA content clearly indicates the TFA concentration dependency of the solubilization of the reactants. The experiments were carried out at the temperature of 40 °C. Right: 0.5 equiv. $ZnCl_2$ were added for these experiments. The legend refers to both graphs.

concentration of TFA (at least 3% (v/v) TFA for 8 $mmol \cdot L^{-1}$ peptide concentration) is necessary for the reaction to take place. The change in reaction rate can be explained by the increased solubilization of the peptide by increasing the TFA concentration. Furthermore, the addition of $ZnCl_2$ accelerates the reaction since it is known that Lewis acids activate the dienophile – in the present case the C=S double bond – by coordination to the sulfur atom.[15] By elevating the lowest unoccupied molecular orbital (LUMO) of the dienophile, it becomes more electrophilic and undergoes the Diels-Alder-reaction with electron rich dienes more readily.[21] Adhering to the philosophy of sustainable chemistry, $ZnCl_2$ as a heavy metal catalyst was omitted in the experiments on the cellulose surfaces. The reaction is also displaying fast conversion without the use of a catalyst.

The influence of temperature was verified by monitoring the reaction progress via SEC-ESI-MS experiments (see **Figure 2**). The reaction shows very little or no dependence on temperature regarding the resulting product (**3**)/reactant (**1**) ratio, which allows for fast conversions at ambient temperature. Nevertheless, increased temperatures should be avoided as they lead to dimerization of the Cp terminated poly(methyl methacrylate) (PMMA-Cp). Inspection of **Figure 3**, which depicts the initial poly(methyl methacrylate) (**2**) molecular weight distributions as well as the resulting oligopeptide-polymer conjugate **3** distributions for three temperatures (i.e. 22 °C, 40 °C and 55 °C) as a function of time, indicates that indeed high molecular weight material at twice the molecular weight of **1** is generated. Thus, it is advisable to work at ambient temperatures to minimize Cp-dimerization processes. It is especially important to note that Cp-dimerization processes are unimportant for the subsequent surface grafting reactions as this process cannot occur in the thioamide functional Cp-cellulose grafting process.

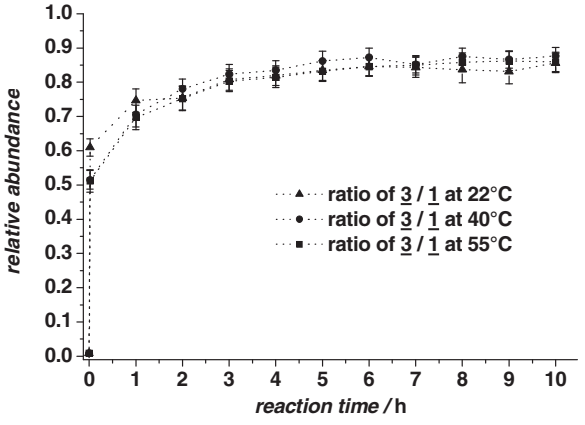

Figure 2. Integration ratio of the product (**3**)/reactant (**1**) signal resulting from a SEC-ESI-MS experiment for the elution time segment between 15.2–16.6 min of three repeating units as a function of the reaction time at different temperatures. The variation of the temperature does – within error – not influence the conversion.

To investigate the HDA reactivity of various Z-groups within the employed thioamides, BPDF as a second HDA-capable thiocarbonyl thio compound was employed. SEC-ESI-MS results indicate that the phosphoryl group is superior regarding conversion despite the fact that the reaction is carried out in the presence of TFA which is known to activate the pyridinyl group. In **Figure 4**a comparison of the conversion to the peptide-PMMA conjugate between thioamide functional oligopeptide bearing a phosphoryl group (Phos-GGFPWWG) and a pyridinyl group (Py-GGFPWWG) is depicted. By comparing the conversion it is evident that the modified BDPDF peptide is reacting faster with the Cp terminated PMMA. Thus, for the subsequent cellulose surface modification, the more reactive phosphoryl thioamide functionalized peptide was used.

To serve as a diene functional surface, cellulose was modified with Cp moieties on its surface (Cel-Cp).[8] We have recently demonstrated that Cp functionalization of cellulose is a versatile and effective route for the decoration with synthetic polymer strands carrying electron deficient dithioesters.[8] To the best of our knowledge, we demonstrate in here for the first time a thioamide-Cp ligation process to modify biopolymer surfaces in a modular fashion. Cp functionalized cellulose was simply shaken in a peptide solution at ambient temperature and subsequently washed to remove physisorbed material. To evidence the effectiveness of the developed ligation reaction on the biosubstrate, the thioamide functionalized model peptide **2** was grafted onto Cel-Cp (**4**) (see **Scheme 4**). High-resolution Fourier transform infrared microscopy (HR-FTIRM) has been

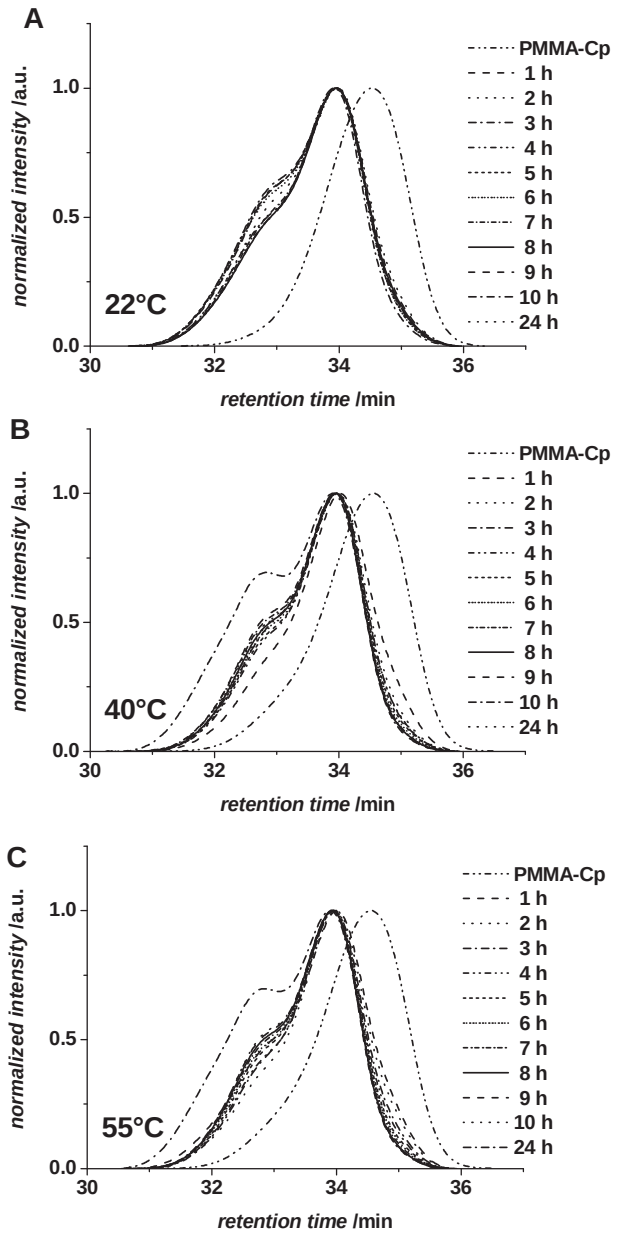

Figure 3. SEC results of the reaction of PMMA-Cp (**1**) (M_n = 2100 g·mol^1, *PDI* = 1.1) with Phos-GGFPWWG (**2**) at variable temperatures (**A**: 22 °C, **B**: 40 °C, **C**: 55 °C) for different reaction times leading to the desired peptide-polymer conjugate **3**. The shoulder at an elution time of 32.7 min indicates that at elevated temperatures a dimerization of PMMA-Cp occurs.

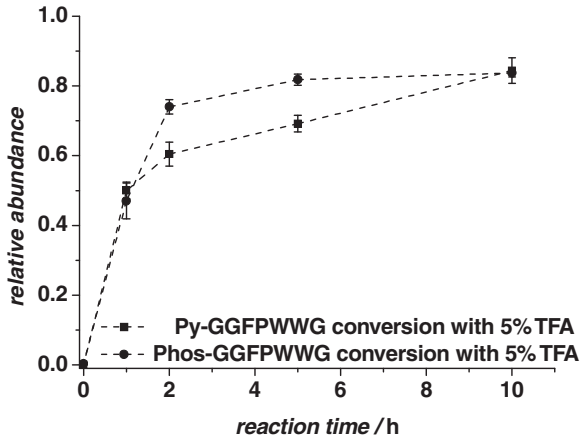

Figure 4. Integration ratio of the peptide-PMMA conjugate/reactant (**1**) signal of the SEC-ESI-MS experiment at the elution time interval between 15.2–16.6 min of three repeating units as a function of the reaction time for the synthesis of peptide-PMMA conjugate by the reaction of PMMA-Cp with Py-GGFPWWG and Phos-GGFPWWG, respectively, in the presence of 5% TFA. The thioamide functional peptide bearing a phosphoryl group (Phos-GGFPWWG) is accelerating the reaction compared to the thioamide functional peptide bearing a pyridinyl group (Py-GGFPWWG).

reported to be a versatile tool to monitor and visualize grafting reactions on various substrates.[8,22] The results acquired via the HR-FTIRM technique evidence – in agreement with other characterization techniques (see below) – successful grafting of thioamide functional peptides onto cellulose (refer to **Figure 5**). On the left hand side the FT-IR images of cellulose grafted with the model peptide (Cel-*g*-GGFPWWG) (**5**) are displayed, depicting in (A) the C-H vibration signal (ν = 950–1200 cm^{-1}) of the cellulose fiber and in C the amide signal (ν = 1600–1710 cm^{-1}) of the grafted peptide. The comparison with the control experiment ((B) and (D)) reveals a clear increase of the carbonyl vibration of **5**. As control reaction sequence, tosylated cellulose (Cel-OTos) was subjected to identical reaction conditions to prove that the analyzed samples only contain covalently linked and not merely physisorbed peptide. Cel-OTos serves as precursor for the subsequent Cp functionalization. The active hydroxyl groups on the biosubstrate surface are transformed into tosylate leaving groups and consecutively converted into the reactive Cp functionalities.[8] Inspection of Figure 5 indicates that the control sequence (lower part) shows no signal for the peptide on the cellulose surface. The HR-FTIRM data thus unambiguously evidence that the robust thioamide-Cp based HDA reaction leads to a covalent tethering of the oligopeptide chains onto the cellulose surface.

To further verify and quantify the successful grafting, several additional characterization methods are employed. XPS analysis is a suitable tool to evidence the modification of biosurfaces due to its high sensitivity.[8] The N 1s spectra for **5** (A) and the control sample (B) are displayed in **Figure 6**. The N 1s signal at 400.3 eV corresponds to the nitrogen of an amide bond.[23] It can be clearly shown that the intensity of the signal of **5** is remarkably higher than in the control sample since the signal/noise ratio is significantly higher. It should be also noted that the peaks shown in Figure 6 are normalized to the highest intensity which only allows for comparison of the signal to noise ratio. The quantitative analysis of the XPS spectra of **5** shows a five-fold increase of the nitrogen signal (3.9 at.%) after the reaction with the model peptide **2** which clearly indicates the successful grafting, since the tosylated cellulose serving in an XPS control experiment shows a significantly lower nitrogen content (0.6 at.%). Cel-Cp contains 3.0 at.% sulfur which are caused by residual tosyl-groups on the cellulose surface (which served as leaving groups in the subsequent Cp functionalization for the preparation of Cel-Cp); the S 2p spectrum (not shown here) shows a doublet with S $2p_{3/2}$ at 168.9 eV as reported in detail

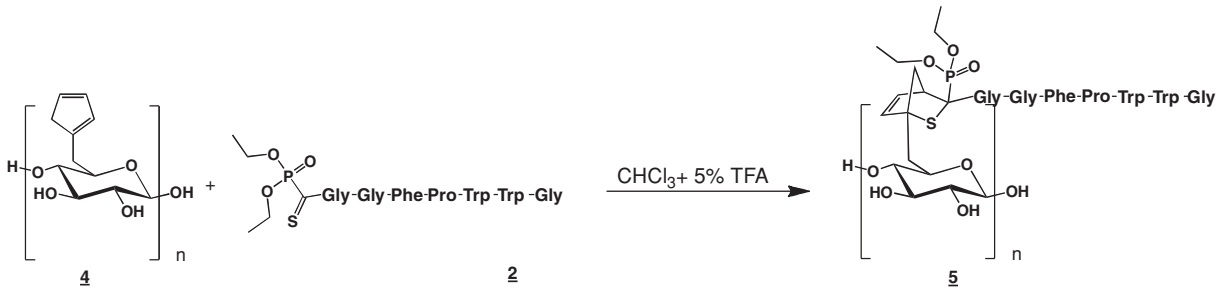

Scheme 4. General strategy for the coupling of the thioamide functional peptide (Phos-GGFPWWG) and cyclopentadienyl functional cellulose surface: Cel-*g*-GGFPWWG as a model system. The same general sequence was applied to the grafting of tritrpticin (see Figure S8 for the structural image of Phos-tritrpticin).

in a previous publication.[8] Little traces of nitrogen, assigned to ethylenediaminetetraacetate (EDTA), are found. EDTA was employed to remove traces of adsorbed nickel after Cp functionalization of the cellulose.

Elemental analysis of **5** underpins the successful peptide grafting sequence (**Table 1**). Elemental analysis offers valuable information of the loading capacity of the sample, as it allows to quantify the amount of grafted peptide. In addition,

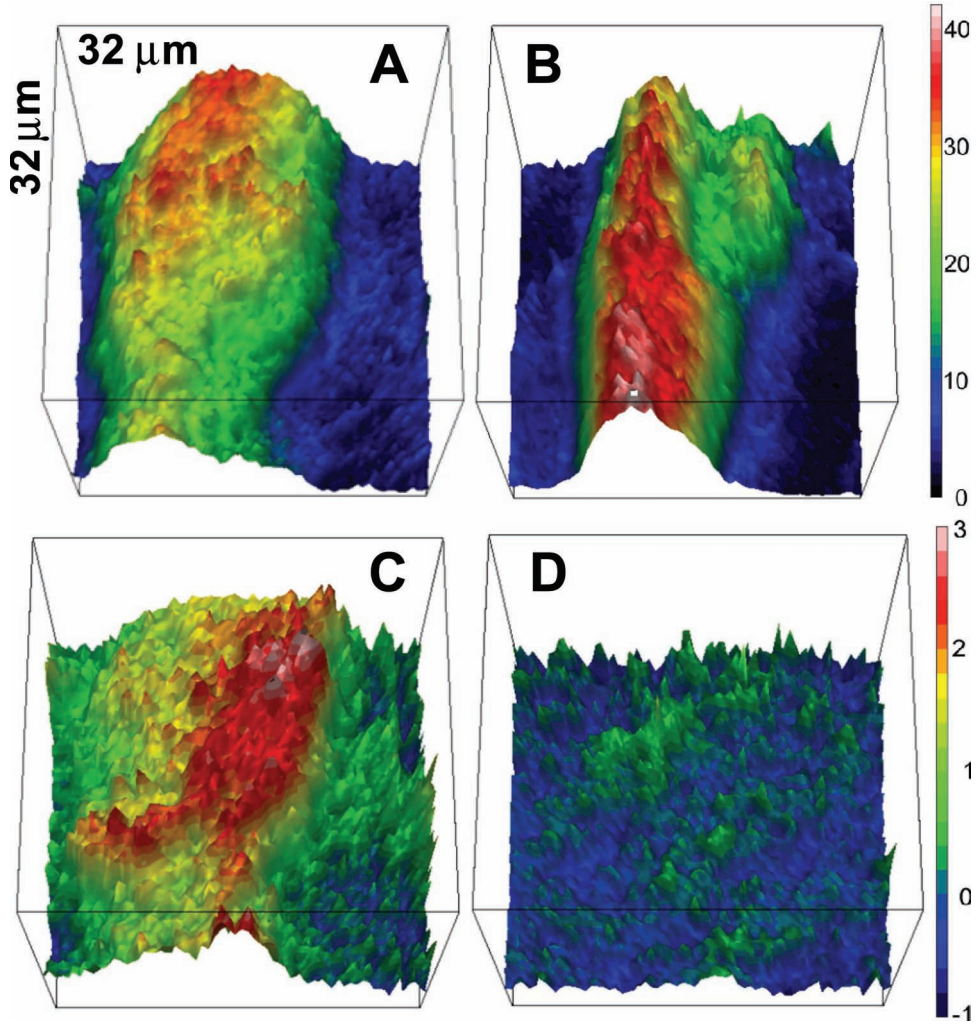

Figure 5. High resolution FT-IR microscopy images of Cel-*g*-GGFPWWG 5 (left: (A) and (C)) and control experiment (right: (B) and (D)). Both 5 and the control sample (tosylated cellulose) were subjected to identical reaction conditions (shaking in $CHCl_3$ with 5% TFA and a concentration of thioamide functional peptide of 36 µmol·mL^{-1} at ambient temperature for 17 h). Comparison of the integration values of cellulose fingerprint vibrations (950–1200 cm^{-1}) of (A) Cel-*g*-GGFPWWG and (B) control experiment and the peptide signal (1600–1710 cm^{-1}) of (C) Cel-*g*-GGFPWWG and (D) control experiment. (Intensity increases from blue to red displayed in the legends on the right side).

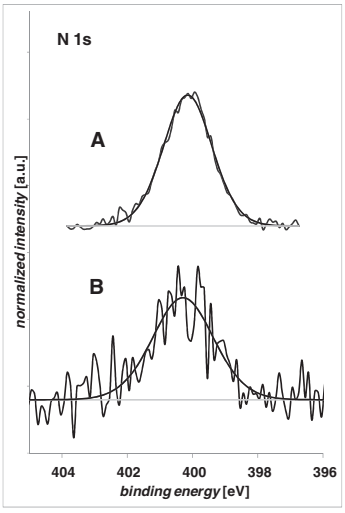

Figure 6. N 1s XPS spectra of Cel-*g*-GGFPWWG (**5**) (A) and the corresponding control sample (B) (Cel-OTos under the same reaction conditions). The nitrogen signal at 400.3 eV corresponds to an amide signal and confirms the peptide coupling on **5**.

5 shows a high nitrogen content of 2.4 at.% which emphasizes the effectiveness of the grafting by comparing this value to the control experiment where no nitrogen is detected. To calculate the loading capacity, the increase in nitrogen content was used as an analytical marker. Assuming that only the increase in nitrogen can be attributed to the addition of the peptide, 17.6 mg nitrogen per gram Cel-*g*-GGFPWWG can be found. **Equation 1** predicts the loading capacity based on the nitrogen content of the employed cellulose material[7a]

$$LC = \frac{W(N)}{n(N)M(N)} \quad (1)$$

where LC is the loading capacity (in $mol \cdot g^{-1}$), $W(N)$ is the weight of nitrogen per 1 g of cellulose substrate obtained by elemental analysis, $n(N)$ is the number of nitrogen atoms per grafted molecule (in the case of GGFPWWG $n(N) = 9$) and $M(N)$ is the molecular weight of nitrogen, leading to a loading capacity of 140 µmol **2** per gram of cellulose for **5**. The loading capacity is comparable to those reported for the grafting onto microspheres. Recently Kaupp et al.[7b] reported loading capacities up to 180 $\mu mol \cdot g^{-1}$ for the grafting of 4-((pyridine-2-carbodithioyl)methyl)benzoic acid onto microspheres. Nebhani et al. functionalized microspheres grafted with polystyrene and quantified the loading capacity to be close to 200 $\mu mol \cdot g^{-1}$.[7a] Thus, the herein reported loading capacity is in line with previously obtained loading capacities via 'grafting-to' approaches. In conclusion, all employed characterization techniques verify that the grafting of the thioamide functionalized model oligopeptide **2** was successful.

Table 1. Elemental analysis results for Cel-*g*-GGFPWWG.

sample	C (wt.%)	O (wt.%)	N (wt.%)	S (wt.%)
Cel-Cp	42.25	47.64	0.67	0.00
Cel-*g*-GGFPWWG	48.87	34.05	2.43	5.12
Control experiment	46.86	39.38	0.00	7.00

It should be stated that although the primary hydroxyl group in C6 position of the cellulose repeating unit shows a higher reactivity, no claim of regioselective surface functionalization is made. Cellulose serves merely as a hydroxyl functional biosupport, whose surface properties are altered by the grafting.

After the successful grafting of the model oligopeptide onto the cellulose substrate, the thioamide functional tritrpticin was employed to modify the cellulose surface. Our motivation for employing tritrpticin as peptide is the desire to use – at a later stage – the generated surface in antibacterial applications.[10] FT-IR measurements of **5** show a distinctive amide vibration in the region of 1600–1710 cm^{-1} corresponding to the peptide (Figure S1). The results of the HR-FTIRM imaging are shown in **Figure 7**. On the left hand side the FT-IR images of Cel-*g*-tritrpticin are displayed, showing in (A) the C-H vibration signal (ν = 950–1200 cm^{-1}) of the cellulose fiber and in (C) the amide signal (ν = 1600–1710 cm^{-1}) of the grafted peptide. The comparison with the control experiment ((B) and (D)) shows an even clearer difference in the amide signal. In comparison with the results of the model peptide, Cel-*g*-tritrpticin has – as expected – a more pronounced amide signal since there are more amino acids linked in tritrpticin forming more amide bonds. The less intense cellulose signal imaged for Cel-*g*-tritrpticin shown in Figure 7A can be explained by the longer peptide chains, covering the cellulose fiber. Therefore the sample has a proportionally higher absorption of the IR radiation compared to the model peptide **5**.

In addition, XPS analysis is employed to characterize the grafting of tritrpticin. In **Figure 8** the N 1s, P 2p, C 1s and S 2p spectra of Cel-*g*-tritrpticin (A) and the precursor Cel-Cp (B) are depicted. It should be noted that all the spectra are again normalized to the peak of highest intensity, allowing for a comparison of ratio changes.

A clear difference can be detected by the comparison of the heteroatom signals. As can be seen in Figure 8, the precursor is bearing little to no nitrogen content on the surface whereas Cel-*g*-tritrpticin is displaying a clear distinctive peak at 400.3 eV which–as stated above–corresponds to nitrogen located in amide moieties. The comparison of the N 1s signal of the Cel-*g*-tritrpticin and of the control sample is shown in Figure S6. The Cel-*g*-tritrpticin spectrum shows a peak with a much better signal to noise ratio than the control sample, evidencing the successful grafting of tritrpticin. Phosphor as second analytical marker supports the successful grafting, too. The Cel-*g*-tritrpticin sample shows a distinctive peak at 133.9 eV which can be assigned to phosphorus in a high oxidation state,[24] whereas in the precursor and the control experiment (see Figure S7) no phosphorus can be detected. To extend the analysis, the carbon signal can be employed. The C 1s signal of (A) shows the increase of the intensity of the peak at 288.3 eV, which is associated with carbon located in an amide moiety.[23] The ratio between the amide carbon compared to the C-OH moiety generated by the cellulose substrate, at 286.6 eV, is increasing. This is to be expected since the conjugation of tritrpticin on the cellulose surface leaves the sample with a large number of amide bound carbon. The peak occurring at 292.6 eV can be assigned to a $C\text{-}F_3$ as it can be found in trifluoroacetic acid, resulting

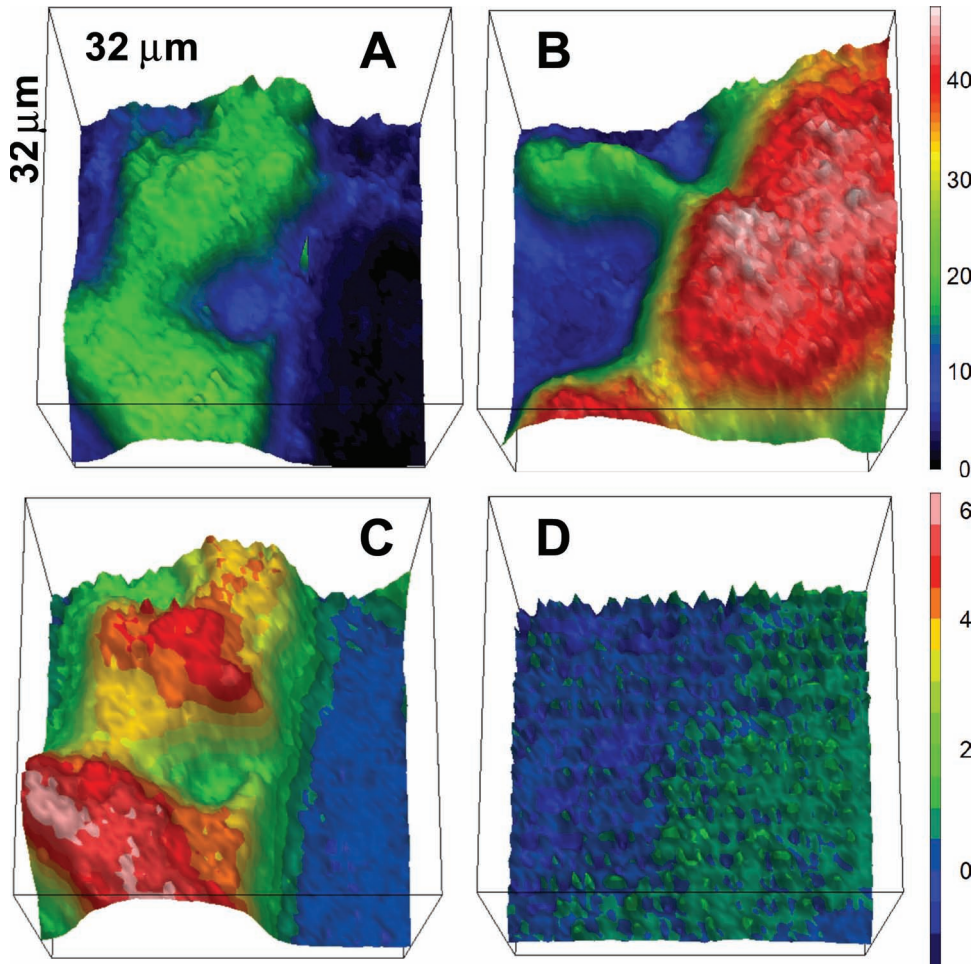

Figure 7. High resolution FT-IR microscopy images of Cel-*g*-tritrpticin (left) and control experiment (right). Both Cel-*g*-tritrpticin and control sample (pretreated cellulose) were subjected the same reaction conditions (shaking in $CHCl_3$ with 5% TFA and a concentration of thioamide functional peptide of 36 µmol·mL^{-1} at ambient temperature for 17 h). Comparison of the integration values of cellulose fingerprint vibrations (950–1200 cm^{-1}) of (A) Cel-*g*-tritrpticin and (B) control experiment and the peptide signal (1600–1710 cm^{-1}) of (C) Cel-*g*-tritrpticin and (D) control experiment. (Intensity increases from blue to red displayed in the legends on the right side).

from salt adducts formed with the peptide (see also below).[23] As fourth elemental species the sulfur signal gives further information. The characteristic S $2p_{3/2}$ doublet peak at 168.7 eV corresponds to sulfur in the oxidation state +VI.[25] Such a high oxidized sulfur content in Cel-Cp is related to the residual tosylate groups on the surface (about the inevitable appearance of tosylate groups, please refer to previous work[8]). On the surface of Cel-*g*-tritrpticin a second species occurs at 162.8 eV which is expected for the C-S/S-H components.[26] Although an oxidation process could be previously observed with these moieties[8] the same species can be prominently found in tritrpticin – which was confirmed via reference measurements (not shown here) – indicating the successful grafting.

The increase of the nitrogen signal is distinctive from 0.2 at.% for Cel-Cp to more than 15 at.% for Cel-*g*-tritrpticin. Even with a higher nitrogen content in the control experiment (3.6 at.%) – pretreated Cel-OH which was subjected the same reaction conditions as Cel-*g*-tritrpticin – it is evident that the grafting was successful since the control experiment contains only one fifth of the nitrogen content compared to the nitrogen content detected in Cel-*g*-tritrpticin. Finally – as stated above – sulfur as C-S/S-H can be found with 0.4 at.% in Cel-*g*-tritrpticin and only 0.1 at.% in the control experiment.

The discrepancy between the missing amide bond in the FT-IR spectra of the control experiment (Figure S1) and the appearance of a substantial amount of nitrogen in the XPS spectrum and the elemental analysis measurements of the control sample can be explained by the chemical composition of tritrpticin. Tritrpticin contains four arginine units featuring four nitrogen atoms per molecule from which only one is in an amide bond. Thus, the ratio of nitrogen content to amide signal in Cel-*g*-tritrpticin differs from the ratio in Cel-*g*-GGFPWWG and therefore cannot be directly compared. Furthermore, fluorine can be found (5.8 at.%) in Cel-*g*-tritrpticin. Due to its high polarity and positive net charge, tritrpticin likely traps traces of trifluoroacetic acid molecules as salt adducts, which are employed for the solubilization of the peptide during the ligation reaction.

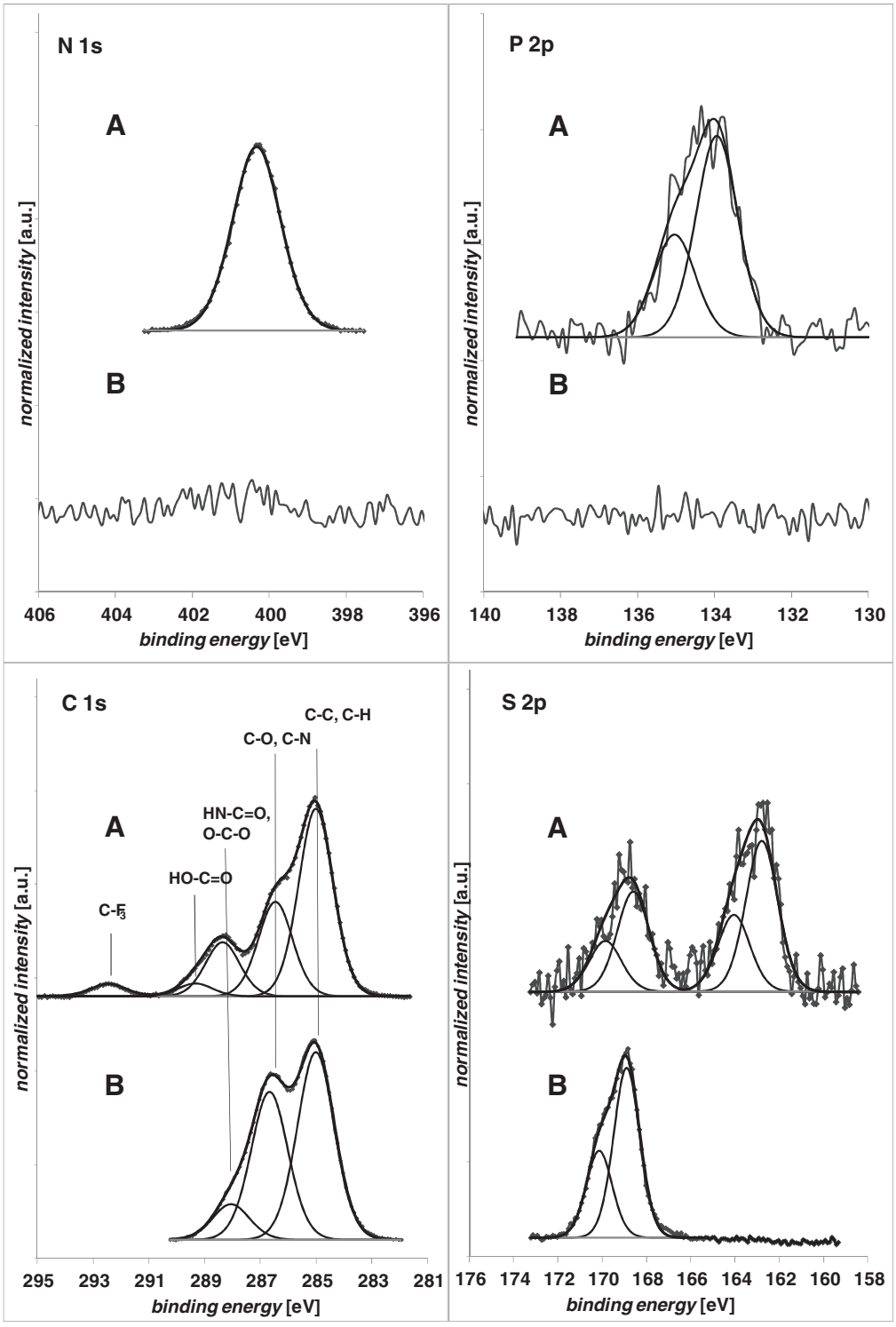

Figure 8. N 1s, P 2p, C 1s, and S 2p XPS spectra of Cel-*g*-tritrpticin **5** (A) and the precursor Cel-Cp (B), which show clearly the grafting of tritrpticin as the introduction of nitrogen, phosphorus and the second sulfur species can be assigned to the grafted tritrpticin (for details see text).

Elemental analysis measurements of Cel-*g*-tritrpticin corroborate the obtained results: The nitrogen content shown in **Table 2** for Cel-*g*-tritrpticin is significantly higher than the nitrogen found in the control experiment. With an increase of over 4 at.% the nitrogen found in Cel-*g*-tritrpticin is undoubtedly supporting the successful grafting. Assuming that only the increase of nitrogen can be attributed to the addition of tritrpticin, 41.4 mg nitrogen per gram Cel-*g*-tritrpticin (corrected

Table 2. Elemental analysis results for Cel-*g*-tritrpticin.

sample	C (wt.%)	O (wt.%)	N (wt.%)	S (wt.%)
Cel-Cp	47.09	41.00	0.26	4.12
Cel-*g*-tritrpticin	47.87	33.73	4.71	2.98
Control experiment	42.46	–*	0.31	0.00

*sample size was insufficient for oxygen determination.

with the control sample results) can be found yielding a loading capacity of 99 µmol of tritrpticin per gram of cellulose for Cel-*g*-tritrpticin. This result is – as expected – lower than the one obtained with the model peptide due to the fact that tritrpticin is sterically much more demanding.

Additionally, the grafting of tritrpticin changes the hydrophobicity of the surface. Whereas Cel-Cp shows hydrophobic behavior (refer to Figure S2) the Cel-*g*-tritrpticin shows more hydrophilic surface properties due to the polar nature of tritrpticin, thus the sample is not repelling water droplets.

3. Conclusions

The successful heterogeneous grafting of variable peptides onto a solid cellulose surface using mild thioamide HDA chemistry is reported. The functionalization of oligopeptides with HDA capable electron deficient thiocarbonyl thio species results in a new class of thioamide functional oligopeptides which can readily undergo [4 + 2] cycloaddition reactions. An in-depth investigation of the influence on the conversion with cyclopentadienyl functional poly(methyl methacrylate) was initially carried out. It was shown that the grafting reaction in solution can be accelerated by using a Lewis acid catalyst such as $ZnCl_2$. The reaction is displaying fast conversion also without Lewis acid catalysis and shows little or no temperature dependence. In addition, it could be demonstrated that in solution the phosphoryl Z-group of the thioamide leads to a more reactive functional oligopeptide than the pyridinyl moiety. The reactions carried out in solution were characterized with SEC and SEC-ESI-MS. The successful "grafting-to" of a model oligopeptide (Phos-GGFPWWG) onto cyclopentadienyl functionalized cellulose was realized as well as the grafting of a functionalized tritrpticin, which is known to have antimicrobial properties in its bound state. The cellulose-peptide hybrid materials were characterized using high resolution FT-IR microscopy, XPS and elemental analysis. The successful grafting of bioactive peptides onto biosurfaces provides access to new fields in tissue engineering, biohybrid materials and modular surface modifications.

4. Experimental Section

The synthesis of Cp functionalized cellulose (4)[8] and cyclopentadienyl terminated PMMA (1)[20] (SEC data provided in Figure S3) and dithioesters[27] are described elsewhere. All other chemicals were used as received.

General procedure for the synthesis of thioamide functional peptides: The peptide synthesis was performed on an Applied Biosystems 433a peptide synthesizer in a 0.1 mmol scale using a TentaGel Standard Rink-Amide Linker (SRAM) resin as solid support. Fmoc-amino acid derivatives were coupled following standard ABI-Fastmoc protocols (no capping, single coupling of amino acid 1-4 and afterwards double coupling) in *N*-Methyl-2-pyrrolidone (NMP) facilitated by 2-(1H-benzotriazol-1-yl)-1,1,3,3-tetramethyluronium hexafluorophosphate (HBTU)/ diisopropyl ethylamine (DIPEA). After final Fmoc removal the resin was transferred to a 40 mL glass reactor with a filter, where BDPDF was coupled three times at ambient temperature: 1) BDPDF (0.2 mmol) and *N*-methylimidazole (NMI) (0.8 mmol) for 2 h, 2) BDPDF (0.2 mmol) and NMI (0.8 mmol) for 15 h, 3) BDPDF (0.3 mmol) and NMI (1.2 mmol) for 3 h. After each step the resin was washed with NMP and subsequently with NMP and dichloromethane (DCM) and dried overnight under vacuum at 25 °C. Cleavage from the resin was performed with TFA/DCM/triethylsilane (TES) 40:57:3 v/v for 2 h, followed by TFA/H_2O/TES 90:8:2 v/v for 2 h to remove the 2,2′,4,6,7-pentamethyldihydro-benzofuran-5-sulfonyl (Pbf) protection groups and to obtain the completely deprotected peptide. The thioamide functionalized peptide was isolated by diethylether precipitation, centrifugation and three times lyophilization from water. Molecular characterization was performed by ESI-MS. (Phos-GGGFPWWG + Na^+: m/z = 1007.3 Da; Phos-tritrpticin + 2 H^+: m/z = 1098.7 Da).

General procedure for the conjugation of thioamide functional peptides with PMMA-Cp in solution: Cyclopentadienyl terminated PMMA (M_n = 2100 Da, *PDI* = 1.1, 13 mmol, 1.0 equiv.) and the thioamide functionalized peptide (19 mmol, 1.5 equiv.) were dissolved in a mixture of $CHCl_3$ and TFA (5 vol.%. if not stated otherwise) and shaken for 15 h at ambient temperature. For the reaction with the addition of a catalyst, $ZnCl_2$ (0.5 equiv.) was added prior to the reagents in the sample vial. After the completion of the reaction, the solvent was evaporated by a N_2-stream.

Synthesis of Cel-g-Peptide: In a 6 mL vial thioamide functionalized peptide (36 µmol) was immersed in a $CHCl_3$/TFA mixture (ratio 0.95:0.05, 1 mL) to give a yellow solution. Cel-Cp (2.0 mg) was added and the solution was allowed to shake at ambient temperature for 17 h. Subsequently the sample was shaken for 150 min in 20 mL $CHCl_3$/TFA (ratio 0.95:0.05) followed by 30 min of shaking in 5 mL THF. Finally the sample was allowed to air-dry. The same reaction procedure was carried out with pretreated cellulose as a control experiment. Refer to reference[8] for the pretreatment protocol.

Size Exclusion Chromatography (SEC): SEC measurements were performed on a Polymer Laboratories (Varian) PL-GPC 50 Plus Integrated System, comprising an autosampler, a PLgel 5 µm beadsize guard column (50 × 7.5 mm) followed by three PLgel 5 µm Mixed-C columns (300 × 7.5 mm) and a differential refractive index detector using THF as the eluent at 35 °C with a flow rate of 1 mL min^{-1}. The SEC system was calibrated using linear poly(styrene) standards ranging from 160 to 6 · 10^6 g mol^{-1} and linear poly(methyl methacrylate) standards ranging from 700 to 2 · 10^6 gmol[1]. Molecular weights relative to PMMA are reported in the current contribution. Calculation of the molecular weight of poly(methyl methacrylate) proceeded via the Mark-Houwink parameters for poly(methyl methacrylate) (K = 12.8 · 10^{-5} dL·g^{-1} and α = 0.69[28]).

Size Exclusion Chromatography-Electrospray Ionization-Mass Spectrometry (SEC-ESI-MS): SEC-ESI-MS spectra were recorded on a LXQ mass spectrometer (ThermoFisher Scientific, San Jose, CA) equipped with an atmospheric pressure ionization source operating in the nebulizer assisted electrospray mode. The instrument was calibrated in the m/z range 195 - 1822 using a standard containing caffeine, Met-Arg-Phe-Ala acetate (MRFA) and a mixture of fluorinated phosphazenes (Ultramark 1621) (all from Aldrich). A constant spray voltage of 6 kV was used and nitrogen at a dimensionless sweep gas flow-rate of 2 (approximately 3 L·min^{-1}) and a dimensionless sheath gas flow-rate of 5 (approximately 0.5 L·min^{-1}) were applied. The capillary voltage, the tube lens offset voltage and the capillary temperature were set to 10 V, 70 V and 275 °C respectively. The LXQ was coupled to a Series 1200 HPLC-

system (Agilent, Santa Clara, CA, USA) consisting of a solvent degasser (G1322A), a binary pump (G1312A), a high-performance autosampler (G1367B), followed by a thermostated column compartment (G1316A). Separation was performed on two mixed bed size exclusion chromatography columns (Polymer Laboratories, Mesopore 250 × 4.6 mm, particle diameter 3 µm) with a precolumn (Mesopore 50 × 4.6 mm) operating at 30 °C. THF at a flow rate of 0.30 mL·min^{-1} was used as eluent. The mass spectrometer was coupled to the column in parallel to a RI-detector (G1362A with SS420x A/D) in a setup described earlier.[11] 0.27 mL·min^{-1} of the eluent were directed through the RI-detector and 30 µL·min^{-1} infused into the electrospray source after postcolumn addition of a 100 µM solution of sodium iodide in methanol at 20 µL·min^{-1} by a micro-flow HPLC syringe pump (Teledyne ISCO, Model 100DM). A 20 µL aliquot of a polymer solution with a concentration of 3 mg·mL^{-1} was injected onto the HPLC system. The following integrations were carried using a spread-sheet number analysis package by applying the principle of area calculation via the trapezoidal rule over several repeating units to minimize ionization bias:

$$Area = \int_a^b f\left(\frac{m}{z}\right) d\frac{m}{z} \approx \Delta\frac{m}{z}\left(\frac{A_0}{2} + A_1 + A_2 + A_3 + \cdots + \frac{A_n}{2}\right)$$

For further details on the integration method and ESI-MS quantification method please refer to reference.[29]

Fourier-Transform (FT)-IR Measurements and FT-IR Microscopy Imaging: Infrared measurements have been performed using a Bruker FT-IR microscope HYPERION 3000 coupled to a research spectrometer VERTEX 80. The HYPERION 3000 microscope is equipped with two types of detector: a single element MCT-detector (Mercury Cadmium Telluride) for the conventional mapping approach and a multi-element FPA-detector (focal plane array) for imaging. The FPA-detector has been used for the laterally resolved measurements. The multi-element FPA-detector consists of 64 × 64 elements allowing for the simultaneous acquisition of 4096 spectra covering a sample area of 32 × 32 µm (for ATR detection). With the FPA-detector in combination with the 20 × Germanium ATR objective, a theoretical lateral pixel resolution of 0.25 µm^2 is achieved. For post-processing a baseline correction and atmospheric compensation were employed.

Elemental Analysis: The elemental composition of the cellulose samples was analyzed using an automatic elemental analyzer Flash EA 1112 from Thermo Scientific, which was equipped with a MAS 200R auto sampler.

X-ray Photoelectron Spectroscopy: XPS investigations were performed on a K-Alpha spectrometer (ThermoFisher Scientific, East Grinstead, UK) using a microfocused, monochromated Al Kα X-ray source (400 µm spot size). The kinetic energy of the electrons was measured by a 180° hemispherical energy analyzer operated in the constant analyzer energy mode (CAE) at 50 eV pass energy for elemental spectra. Data acquisition and processing using the Thermo Avantage software is described elsewhere.[30] The spectra were fitted with one or more Voigt profiles (BE uncertainty: +/–0.2 eV). The analyzer transmission function, Scofield[31] sensitivity factors and effective attenuation lengths (EALs) for photoelectrons were applied for quantification. EALs were calculated using the standard TPP-2M formalism. All spectra were referenced to the C1s peak of hydrocarbon at 285.0 eV binding energy controlled by means of the well known photoelectron peaks of metallic Cu, Ag and Au respectively.

Supporting Information

Supporting Information is available from the Wiley Online library or from the author.

Acknowledgements

C. B.-K. and H. G. B. acknowledge financial support for the current project from the German Research Council (DFG) (BA 3751/12-1). In addition, C. B.-K. acknowledges long term funding from the Karlsruhe Institute of Technology (KIT) in the context of the *Excellence Initiative* for leading German universities as well as the German Research Council (DFG) and the Ministry of Science and Arts of the state of Baden-Württemberg. The authors thank the Fraunhofer Institute for Chemical Technology, Pfinztal, for the elemental analysis measurements and Corinna Preuss (KIT) for help with the evaluation of the XPS data.

Received: January 28, 2012
Revised: April 20, 2012
Published online: June 4, 2012

[1] a) T. Heinze, *Macromol. Symp.* **2009**, *280*, 15–27; b) T. Heinze, T. Liebert, *Prog. Polym. Sci.* **2001**, *26*, 1689–1762; c) D. Roy, M. Semsarilar, J. T. Guthrie, S. Perrier, *Chem. Soc. Rev.* **2009**, *38*, 2046–2064.
[2] a) C.-F. Liu, A.-P. Zhang, W.-Y. Li, F.-X. Yue, R.-C. Sun, *J. Agric. Food Chem.* **2009**, *57*, 1814–1820; b) K. Furuhata, *Carbohydr. Polym.* **1995**, *26*, 25–29; c) M. A. Hussain, T. Liebert, T. Heinze, *Macromol. Rapid Commun.* **2004**, *25*, 916–920.
[3] a) G.-L. Zhao, J. Hafrén, L. Deiana, A. Córdova, *Macromol. Rapid Commun.* **2010**, *31*, 740–744; b) M. Krouit, J. Bras, M. Belgacem, *Eur. Polym. J.* **2008**, *44*, 4074–4081.
[4] E. Malmström, A. Carlmark, unpublished.
[5] a) P. Månsson, L. Westfelt, *J. Polym. Sci.: Part A: Polym. Chem.* **1981**, *19*, 1509–1515; b) C. J. Biermann, J. B. Chung, R. Narayan, *Macromolecules* **1987**, *20*, 954–957; c) N. Tsubokawa, T. Iida, T. Takayama, *J. Appl. Polym. Sci.* **2000**, *75*, 515–522; d) J. Hentschel, K. Bleek, O. Ernst, J.-F. Lutz, H. G. Börner, *Macromolecules* **2008**, *41*, 1073–1075.
[6] a) M. Barsbay, O. Güven, T. P. Davis, C. Barner-Kowollik, L. Barner, *Polymer* **2009**, *50*, 973–982; b) M. Barsbay, O. Güven, M. H. Stenzel, T. P. Davis, C. Barner-Kowollik, L. Barner, *Macromolecules* **2007**, *40*, 7140–7147; c) A. Carlmark, E. Malmström, *J. Am. Chem. Soc.* **2002**, *124*, 900–901; d) A. Carlmark, E. E. Malmström, *Biomacromolecules* **2003**, *4*, 1740–1745; e) D. Roy, J. T. Guthrie, S. Perrier, *Macromolecules* **2005**, *38*, 10363–10372.
[7] a) L. Nebhani, D. Schmiedl, L. Barner, C. Barner-Kowollik, *Adv. Funct. Mater.* **2010**, *20*, 2010–2020; b) M. Kaupp, A. P. Vogt, J. C. Natterodt, V. Trouillet, T. Gruendling, T. Hofe, L. Barner, C. Barner-Kowollik, unpublished.
[8] A. S. Goldmann, T. Tischer, L. Barner, M. Bruns, C. Barner-Kowollik, *Biomacromolecules* **2011**, *12*, 1137–1145.
[9] M. G. J. ten Cate, H. Rettig, K. Bernhardt, H. G. Börner, *Macromolecules* **2005**, *38*, 10643–10649.
[10] M. L. Becker, J. Liu, K. L. Wooley, *Biomacromolecules* **2004**, *6*, 220–228.
[11] D. Klemm, B. Heublein, H. P. Fink, A. Bohn, *Angew. Chem., Int. Ed.* **2005**, *44*, 3358–3393.
[12] a) I. Siró, D. Plackett, *Cellulose* **2010**, *17*, 459–494; b) P. Stenstad, M. Andresen, B. S. Tanem, P. Stenius, *Cellulose* **2007**, *15*, 35–45.
[13] D. Klemm, F. Kramer, S. Moritz, T. Lindström, M. Ankerfors, D. Gray, A. Dorris, *Angew. Chem., Int. Ed.* **2011**, 2–31.
[14] G. Moad, D. H. Solomon, *The Chemistry of Radical Polymerization*, 2nd edition, Elsevier Ltd, Oxford **2006**.
[15] A. J. Inglis, S. Sinnwell, T. P. Davis, C. Barner-Kowollik, M. H. Stenzel, *Macromolecules* **2008**, *41*, 4120–4126.
[16] S. Sinnwell, A. J. Inglis, M. H. Stenzel, C. Barner-Kowollik, *Macromol. Rapid Commun.* **2008**, *29*, 1090–1096.
[17] L. Nebhani, P. Gerstel, P. Atanasova, M. Bruns, C. Barner-Kowollik, *J. Polym. Sci.: Part A: Polym. Chem.* **2009**, *47*, 7090–7095.
[18] L. Nebhani, S. Sinnwell, A. J. Inglis, M. H. Stenzel, C. Barner-Kowollik, L. Barner, *Macromol. Rapid Commun.* **2008**, *29*, 1431–1437.

[19] a) A. J. Inglis, M. H. Stenzel, C. Barner-Kowollik, *Macromol. Rapid Commun.* **2009**, *30*, 1792–1798; b) L. Nebhani, S. Sinnwell, C. Y. Lin, M. L. Coote, M. H. Stenzel, C. Barner-Kowollik, *J. Polym. Sci.: Part A: Polym. Chem.* **2009**, *47*, 6053–6071; c) A. Inglis, S. Sinnwell, M. Stenzel, C. Barner-Kowollik, *Angew. Chem., Int. Ed.* **2009**, *48*, 2411–2414.
[20] A. J. Inglis, T. Paulöhrl, C. Barner-Kowollik, *Macromolecules* **2010**, *43*, 33–36.
[21] S. Danishefsky, E. Larson, D. Askin, N. Kato, *J. Am. Chem. Soc.* **1985**, *107*, 1246–1255.
[22] S. Hansson, T. Tischer, A. S. Goldmann, A. Carlmark, C. Barner-Kowollik, E. Malmström, *Polym. Chem.* **2012**, *1500*, 10–12.
[23] E. Jagst, *Surface Functional Group Characterization Using Chemical Derivatization X-ray Photoelectron Spectroscopy (CD-XPS)*, BAM, Berlin, Germany **2010**.
[24] I. F. Amaral, P. L. Granja, M. A. Barbosa, *J. Biomater. Sci., Polym. Ed.* **2005**, *16*, 1575–1593.
[25] H. Hintz, H.-J. Egelhaaf, H. Peisert, T. Chassé, *Polym. Degrad. Stab.* **2010**, *95*, 818.
[26] L.-P. Wang, Y.-P. Wang, K. Yuan, Z.-Q. Lei, *Polym. Adv. Technol.* **2008**, *19*, 285–290.
[27] I. Abrunhosa, M. Gulea, S. Masson, *Synthesis* **2004**, 928–934.
[28] M. Stickler, D. Panke, W. Wunderlich, *Makromol. Chem.* **1987**, *188*, 2651–2664.
[29] S. P. S. Koo, T. Junkers, C. Barner-Kowollik, *Macromolecules* **2008**, *42*, 62–69.
[30] K. L. Parry, A. G. Shard, R. D. Short, R. G. White, J. D. Whittle, A. Wright, *Surf. Interface Anal.* **2006**, *38*, 1497–1504.
[31] J. H. Scofield, *J. Electron Spectrosc. Relat. Phenom.* **1976**, *8*, 129–137.